Pressure induced structural, electronic topological, and semiconductor to metal transition in AgBiSe2

V. Rajaji, Pallavi S. Malavi, Sharma S. R. K. C. Yamijala, Y. A. Sorb, Utpal Dutta, Satya N. Guin, B. Joseph, Swapan K. Pati, S. Karmakar, Kanishka Biswas, and Chandrabhas Narayana

Pressure induced structural, electronic topological, and semiconductor to metal transition in AgBiSe$_2$

V. Rajaji,[1] Pallavi S. Malavi,[2] Sharma S. R. K. C. Yamijala,[1] Y. A. Sorb,[1] Utpal Dutta,[2] Satya N. Guin,[3] B. Joseph,[4] Swapan K. Pati,[5] S. Karmakar,[2] Kanishka Biswas,[3] and Chandrabhas Narayana[1,a)]

[1]Chemistry and Physics of Materials Unit, Jawaharlal Nehru Centre for Advanced Scientific Research, Jakkur, Bangalore 560 064, India
[2]HP&SRPD, Bhabha Atomic Research Centre, Trombay, Mumbai 400 085, India
[3]New Chemistry Unit, Jawaharlal Nehru Centre for Advanced Scientific Research, Jakkur, Bangalore 560 064, India
[4]Elettra Sincrotrone Trieste, S.S. 14, Km 163.5 in Area Science Park, Basovizza, Trieste 34149, Italy
[5]Theoretical Sciences Unit, Jawaharlal Nehru Centre for Advanced Scientific Research, Bangalore 560064, India

We report the effect of strong spin orbit coupling inducing electronic topological and semiconductor to metal transitions on the thermoelectric material AgBiSe$_2$ at high pressures. The synchrotron X-ray diffraction and the Raman scattering measurement provide evidence for a pressure induced structural transition from hexagonal (α-AgBiSe$_2$) to rhombohedral (β-AgBiSe$_2$) at a relatively very low pressure of around 0.7 GPa. The sudden drop in the electrical resistivity and clear anomalous changes in the Raman line width of the A$_{1g}$ and E$_g^{(1)}$ modes around 2.8 GPa was observed suggesting a pressure induced electronic topological transition. On further increasing the pressure, anomalous pressure dependence of phonon (A$_{1g}$ and E$_g^{(1)}$) frequencies and line widths along with the observed temperature dependent electrical resistivity show a pressure induced semiconductor to metal transition above 7.0 GPa in β-AgBiSe$_2$. First principles theoretical calculations reveal that the metallic character of β-AgBiSe$_2$ is induced mainly due to redistributions of the density of states (p orbitals of Bi and Se) near to the Fermi level. Based on its pressure induced multiple electronic transitions, we propose that AgBiSe$_2$ is a potential candidate for the good thermoelectric performance and pressure switches at high pressure. *Published by AIP Publishing.* [http://dx.doi.org/10.1063/1.4966275]

Recently, there has been an increased research interest in the high pressure studies of semiconducting materials with strong spin orbit coupling (SOC) because they exhibit exotic features such as electronic topological transition (ETT),[1–3] metal insulator transition (MIT),[4,5] topological quantum phase transition (TQPT),[6] structural phase transition, and superconductivity.[7,8] Among these, ETT is one of the technologically important phenomena due to its ability of enhancement in thermoelectric (TE) power.[9,10] Thermodynamically, ETT is a second order isostructural transition without volume collapse and no change in its Wyckoff position.[11] ETT is mainly caused by drastic changes in the topology of the electronic Fermi surface, and the most direct tool to detect is the angle resolved photoemission spectroscopy (ARPES), which shows the changes in the electronic band structure of the materials.[12] But, there is no sophisticated technique to implement the ARPES study under high pressure. Since ETT causes significant changes in transport properties, it can be identified indirectly through changes in the resistivity and the TE power measurements.[4,5,9] ETT can also be detected by Raman line width studies due to the electron-phonon coupling.[1–3,11,13] The pressure induced semiconductor to metal transition is another interesting phenomenon, which is caused by the charge density redistribution during overlapping of atomic orbitals. Electrical resistivity and the Raman line width study are influenced by the semiconductor to metal transition.[14,15]

AgBiSe$_2$ is a narrow band gap ($\sim$0.6 eV) semiconductor, which crystallizes in ordered hexagonal structure (SG: P-3m1, Z = 3) at ambient conditions and shows an intriguing temperature dependent structural order-disorder phase transition behavior.[16,17] The bulk form of AgBiSe$_2$ exhibits the high thermoelectric figure of merit (ZT) of $\sim$1 due to intrinsic low lattice thermal conductivity caused by bond anharmonicity[16] and it shows n-type conduction when doped with Nb and halogen.[16,17] Nanocrystalline AgBiSe$_2$ shows p-n-p type conduction switching during structural phase transition.[18] The presence of strong SOC in AgBiSe$_2$ and its symmetrical equivalence (-3m1) with the binary layered 3D topological insulator (TI) α-Bi$_2$Se$_3$(SG: R-3m, Z = 1) have motivated us to check if AgBiSe$_2$ too exhibit an identical behavior under high pressure. The knowledge of its characteristics under pressure may be useful for the fabrication of a thermoelectric device operating in the mechanically strained environment. In this work, we have investigated pressure dependent synchrotron powder X-ray diffraction (XRD), electrical resistivity, Raman scattering measurements, and first principles calculations up to a maximum pressure of around 21 GPa on AgBiSe$_2$ and observed three transitions, namely, structural transition at 0.7 GPa, ETT around 2.8 GPa, and semiconductor to metal transition above 7.0 GPa.

High purity polycrystalline AgBiSe$_2$ was synthesized by the elemental melting reaction, mixing appropriate ratios of

a)Author to whom correspondence should be addressed. Electronic mail: cbhasi@gmail.com

high-purity elements Ag, Bi, and Se in a quartz tube. The synthesis details are published elsewhere.[17] The pressure was generated by the Mao Bell type diamond anvil cell (DAC) with diamonds of culet size of $400\,\mu m$. The high pressure powder XRD measurement was carried out up to $\sim$12 GPa at the XRD1 beam line of the ELETTRA synchrotron radiation, using a monochromatic beam of wavelength $0.7000\,\text{Å}$ (see details in the supplementary material). The Raman spectra were recorded in the custom-built Raman spectrometer equipped with a diode pumped, frequency-doubled, Nd:YAG solid state green laser with 532 nm wavelength, a SPEX TRIAX 550 monochromator, and a liquid nitrogen cooled CCD detector.[19] The pressure dependence of resistivity at room temperature and at low temperature down to 170 K has been performed on a pressed pellet of the $AgBiSe_2$ sample (of diameter $\sim$50 μm and $\sim$20 μm thick) up to $\sim$12 GPa using a miniature DAC mounted in an optical cryostat. The computational details are given in the supplementary material.

The α-$AgBiSe_2$ compound crystallizes in hexagonal structure with space group P-$3m1$ and the triple primitive hexagonal unit cell as shown in Fig. 1(a), which also shows the indexing and profile matching of the synchrotron XRD pattern at $\sim$0.12 GPa. The calculated lattice parameter values for the α-$AgBiSe_2$ are $a = 4.1886\,\text{Å}$, $c = 19.6540\,\text{Å}$, and $V = 298.61\,\text{Å}^3$. Since the texture affects the obtained XRD pattern strongly, the refined atomic fractional coordinates are considered unreliable. Hence, only the lattice parameters were extracted with the permitted error. The representative
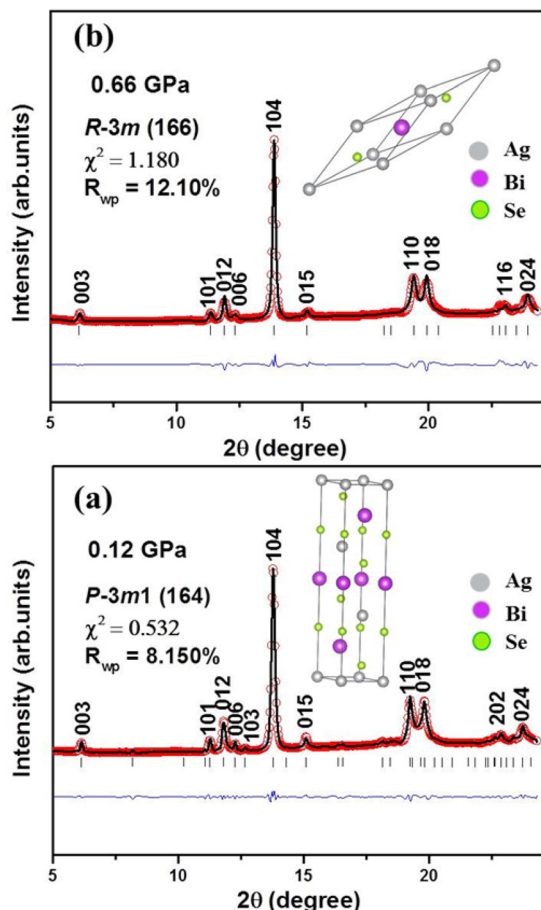
XRD patterns of $AgBiSe_2$ at various pressures are shown in Fig. S1 of the supplementary material. It is evident, from Fig. 1(b), that at 0.7 GPa, α-$AgBiSe_2$ undergoes a structural phase transition from hexagonal (SG: P-$3m1$, $Z = 3$) to rhombohedral (S.G: R-$3m$, $Z = 1$) called here as β-$AgBiSe_2$, which is structurally identical to the 3D topological insulator Bi_2Se_3.[3]

The β-$AgBiSe_2$ contains four atoms in the unit cell, and each Ag/Bi layer is stacked between the two Se layers, as shown in Fig. 1(b). At $\sim$0.66 GPa, one Bragg reflection (103) disappears, and the remaining reflection satisfies the condition $(-h + k + l = 3n)$ of rhombohedral symmetry (R-3m), which is the clear indication of the symmetry change. The pressure-volume curves for the β-$AgBiSe_2$ phase were fitted using a third-order Birch-Murnaghan equation of state (BM-EOS) as shown in Fig. S2 of the supplementary material. The BM-EOS fit yields the bulk modulus, $B_0 = 50.79$ GPa, its pressure derivative, $B_0' = 7.79$, and volume $V_0 = 295.83\,\text{Å}^3$ at zero pressure. Table SI (see supplementary material) summarizes the structural and EOS fit parameters of α-$AgBiSe_2$ and β-$AgBiSe_2$.

The pressure dependent electrical resistivity of $AgBiSe_2$ up to 11.5 GPa at room temperature is shown in Fig. 2. The inset shows the Arrhenius plot (1/T vs ln(R)) of the sample in the range of 170–300 K for a few representative pressures. The value of resistivity is 19.225 mΩ cm at ambient conditions, and the obtained results have been found to be in good agreement with Pan *et al.*[16] It is evident, from Fig. 2, that as the pressure increases, the resistivity of the sample decreases up to 2.8 GPa, with a sudden drop occurring and shows a similar trend to that reported for 3D topological insulator Bi_2Se_3 and Bi_2Te_3. By comparing these results, the observed anomaly at 2.8 GPa in our case can be attributed to an ETT.[4,5] It occurs, when the external perturbations like pressure, chemical doping, temperature, etc., in metals or degenerate semiconductors, leading to the crossing of van Hove singularity (band extremum in the DOS) through the Fermi level, and consequently, the strong redistribution of electrons

FIG. 1. Le Bail fit to the synchrotron XRD pattern for (a) α-$AgBiSe_2$ and (b) β-$AgBiSe_2$.
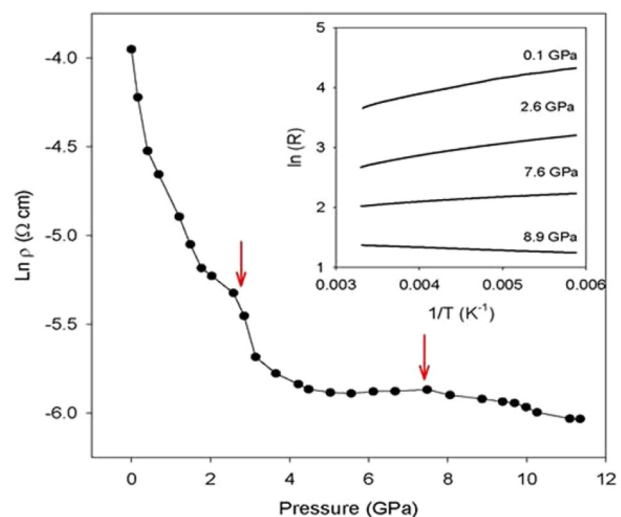

FIG. 2. Pressure dependent electrical resistivity of $AgBiSe_2$ at room temperature condition. The solid red arrow indicates the presence of an ETT at $\sim$2.8 GPa and semiconductor to metal transition above 7.0 GPa. The inset shows the Arrhenius plot of $AgBiSe_2$ at various selected pressure values.

takes place near to Fermi surface.[5,20] Hence, the Fermi surface can undergo different types of topological transition (changes) like appearance and disappearance of void, formation and disruption of a neck, depending on the type of critical point passing through the Fermi surface. Figure 2 shows the systematic decrease in the overall resistance of the sample at high pressure, and the system undergoes metallization in the pressure above 7 GPa where the resistance slope changes from an activation type to the metallic character (see inset of Fig. 2).

Raman spectroscopic studies were undertaken to substantiate the above observations. The factor group analysis for the α-AgBiSe$_2$ structure predicts the ten Raman active phonon modes at the Γ point of the Brillouin zone, Γ = 5 A$_{1g}$ + 5 E$_g$. We have calculated the Raman spectra of α-AgBiSe$_2$ based on the density functional perturbation theory and tentatively assigned the Raman modes as shown in the Table SII (see supplementary material). We observed two Raman active modes namely, A$_{1g}$ and E$_g^{(2)}$ above 100 cm^{-1} in our experiment (see Fig. S3), which are matching well with that observed in Ref. 18. The phonon modes are fitted by the Lorentzian line shape function. The doubly degenerate E$_g^{(2)}$ mode is related to shear vibration along the a-b plane, and the A$_{1g}$ mode can be related to out of plane vibrations along the c axis [see Figs. S4(a), S4(b), and S4(c)]. Figure S5 shows the pressure evolution of Raman spectra up to 20.7 GPa. Upon increasing pressure, a new phonon mode occurs at 0.7 GPa, and this is consistent with the XRD results that AgBiSe$_2$ undergoes a structural transition from hexagonal (*P*-3m1) to rhombohedral (*R*-3m). The newly appeared phonon mode in β-AgBiSe$_2$ phase is assigned to E$_g^{(1)}$ symmetry based on structurally similar compounds α-Bi$_2$Se$_3$ and PdCoO$_2$.[3,21]

The pressure dependence of the frequency of phonon modes for AgBiSe$_2$ is shown in Fig. 3(a). Upon increasing pressure, the E$_g^{(2)}$ mode hardens, and it disappears at 1.19 GPa. The phonon mode A$_{1g}$ initially softens up to 0.7 GPa and thereafter it hardens up to ∼20.7 GPa, which is the maximum pressure reached in Raman study, with a small change in the slope at around 7 GPa. Similarly, the newly appeared phonon mode E$_g^{(1)}$ hardens with pressure up to ∼20.7 GPa, with a slope change at around 7 GPa. The pressure dependent behavior of E$_g^{(2)}$, A$_{1g}$, and E$_g^{(1)}$ modes are fitted by a linear equation, and the calculated pressure coefficients are summarized in Table I.[3] The clear change in the slope of A$_{1g}$ mode around 0.7 GPa with the absence of frequency discontinuity during the structural transition, along with the appearance (E$_g^{(1)}$) and disappearance (E$_g^{(2)}$) of modes confirms it is weakly first order in nature. This is consistent with a very low volume change (∼1.14%) across this transition as seen from the XRD measurements.

At ambient conditions, the line width of A$_{1g}$ and E$_g^{(2)}$ modes are 11.5 cm^{-1} and 8.6 cm^{-1}, respectively. The large line width of the first order A$_{1g}$ mode can possibly be due to the strong phonon-phonon interaction leading to anharmonic decay, which decreases the phonon lifetime as shown in Fig. 3(b).[22] The line width of A$_{1g}$ mode increases up to ∼2.8 GPa and turns around and decreases up to 10.5 GPa with a noticeable change in the slope at ∼7 GPa. In contrast, the line width of E$_g^{(1)}$ mode decreases with pressure up to 2.8 GPa
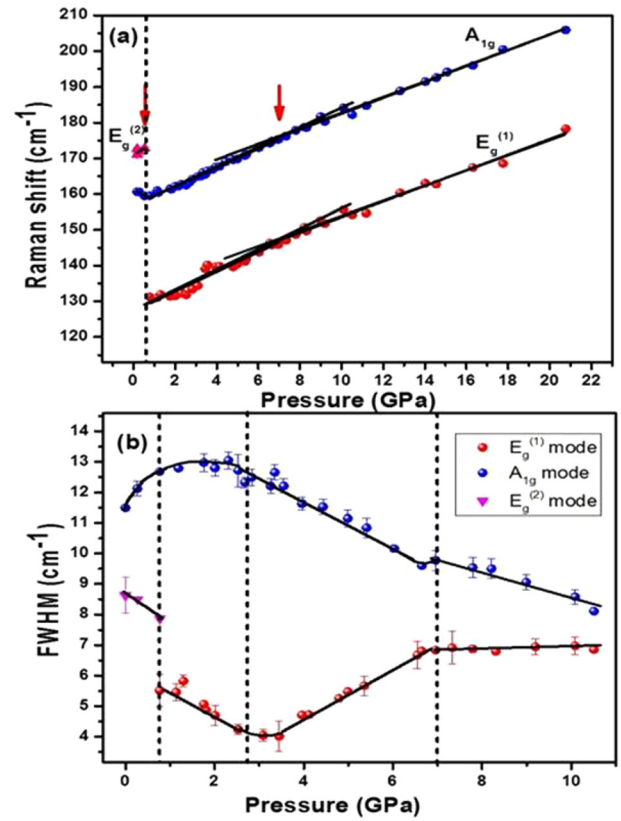

FIG. 3. (a). Pressure versus Raman frequency of A$_{1g}$, E$_g^{(1)}$, and E$_g^{(2)}$ modes of AgBiSe$_2$ up to 20.7 GPa. The black solid line denotes the linear fit to experimental data points. A vertical dotted line at 0.7 GPa denotes the symmetry change from hexagonal (P-*3m*1) to rhombohedral (R-*3m*). A red downward vertical arrow at 7 GPa denotes semiconductor to metal transition. (b). Pressure versus FWHM of the A$_{1g}$, E$_g^{(1)}$, and E$_g^{(2)}$ modes of AgBiSe$_2$ up to 10.5 GPa. The black solid line represents the guide to an eye. The vertical dotted line represents the structural, ETT, and semiconductor to metal transition at ∼0.7 GPa, ∼2.8 GPa, and ∼7.0 GPa, respectively.

and suddenly reverses by broadening up to 7 GPa where it again shows a slope change in the FWHM. The anomalies in the line width of A$_{1g}$ and E$_g^{(1)}$ phonon mode at 2.8 GPa and 7 GPa are consistent with the observations in the resistivity measurements. The Raman changes at 2.8 GPa confirm the pressure induced ETT through electron-phonon coupling in β-AgBiSe$_2$. A detailed comparison between the pressure coefficients and the line width behaviors of β-AgBiSe$_2$ with α-Bi$_2$Se$_3$ is commented in the supplementary material. There is an abrupt change observed in the pressure coefficient of Raman frequency and the line width of the A$_{1g}$ and E$_g^{(1)}$

TABLE I. Pressure dependence behavior of various Raman-mode frequencies of AgBiSe$_2$. The pressure coefficients for α-AgBiSe$_2$ and β-AgBiSe$_2$ were fitted using linear equation $\omega(P) = \omega(P_0) + a_1(P - P_0)$. The superscripts a, b, and c represent the estimation of values at P$_0$ = 1 atm, P$_0$ = 0.7 GPa, and P$_0$ = 7.0 GPa, respectively.

Phase	Raman mode	$\omega(P_0)$ (cm^{-1})	a_1 (cm^{-1} GPa^{-1})
α-AgBiSe$_2$	A$_{1g}$	160.8 ± 0.1[a]	−2.52 ± 0.35[a]
	E$_g^{(2)}$	171.1 ± 0.1[a]	3.06 ± 0.24[a]
β-AgBiSe$_2$	E$_g^{(1)}$	127.3 ± 0.7[b]	2.75 ± 0.17[b]
	E$_g^{(1)}$	131.8 ± 0.8[c]	2.18 ± 0.07[c]
	A$_{1g}$	156.8 ± 0.2[b]	2.64 ± 0.05[b]
	A$_{1g}$	160.4 ± 0.6[c]	2.21 ± 0.05[c]

modes above ∼7 GPa, and this can be attributed to the semiconductor to metal transition. Due to the change in the electronic structure across this transition, the electron-phonon coupling is affected leading to change in the life time as well as the frequency of both A_{1g} and $E_{1g}^{(1)}$ modes.

To understand the reason behind the experimentally observed pressure induced semiconductor to metal transition in β-AgBiSe$_2$, we have performed the first principle calculations. At first, we have studied the changes in band structure (along the Γ-Z-F-Γ-L path) and projected density of states (PDOS) at various pressures (between 0 GPa to 20 GPa), please note that we have considered the rhombohedral structure (β-AgBiSe$_2$) at 0 GPa. The band structure plot for various pressure values are given in the Figs. S6 and S7. Clearly, at zero pressure, the system behaves as a semiconductor with an indirect band gap of ∼0.26 eV as shown in Fig. S6(a). In Figs. 4(a) and 4(b), we have given the PDOS plots at 0 GPa and 20 GPa pressures (for other pressure values, see Fig. S8 in supplementary material). With the increase in pressure, bands near the Fermi level shifts down in energy, suggesting an increased stability for the electrons occupying these bands. Interestingly, the conduction band slowly shifts down with pressure; at ∼11.0 GPa (see Fig. S7(c) in supplementary material), it touches the Fermi-level at Γ-point, and at higher pressures, it is dispersed across the Fermi level, reminiscent of metallic band. Also, from the PDOS plots at 0 GPa and 20 GPa pressures (Figs. 4(a) and 4(b)), it is clear that there is a strong redistribution of DOS near the Fermi level, where, the major redistribution is in the energy states corresponding to p-orbitals of both Se and Bi atoms. See supplementary material for HSE (Heyd-Scuseria-Ernzerhof) results.

As major changes in the band structure near the Fermi level are mainly due to the conduction band, we have plotted the second derivative of change in the conduction band energy with respect to the Fermi-level as a function of
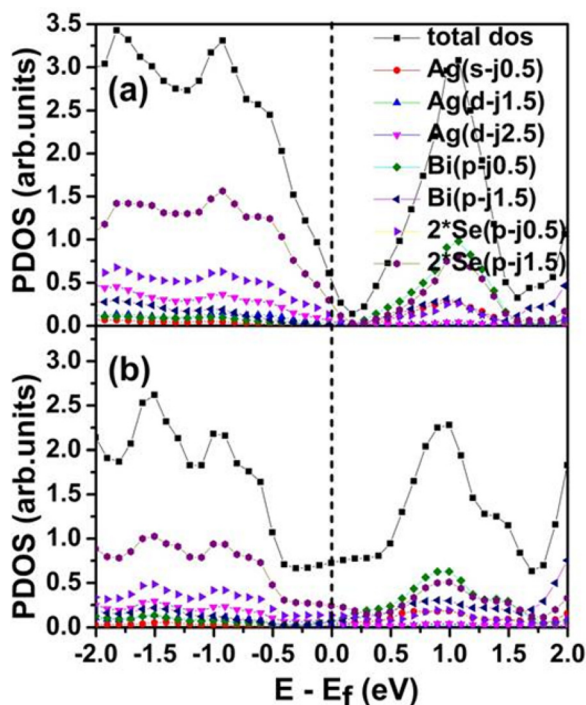
pressure (see Fig. 5) to look clearly whether there is a change in the slope or kink in conduction band energy as a function of wave vector (k). The second derivative of energy would correspond to the electrical conductivity, which is a second-order transport quantity. Figure 5 shows major changes in the regions between 2 to 2.5 GPa and between 11 to 12 GPa. Any changes in the topology of Fermi surface will directly affect the electronic DOS near to the Fermi level and have strong influences on the bands lying very close to the Fermi level. Hence, the inflection point observed at 2 GPa is possibly due to an ETT. Another inflection point observed at 11.5 GPa signifies the overlap of conduction band with Fermi level, where the system starts behaving like metal. To see the effect of exchange-correlation functional on the observed mismatch between the transition pressures from theory and experiment, we have performed the calculations with HSE06 functional, and the results are shown in Figs. S11(a) and S11(b). The exact trend for both HSE06 and Perdew-Burke-Ernzerhof (PBE) functionals suggests that the mismatch is not due to the functional. The density functional theory (DFT) level of theory may not quantitatively match with the experimental data. In fact, since this happens for high pressure, it is due to some nonlinear response, which the DFT fails to capture. It is hard to compare the second order experimental response functions with data from the DFT level of theory. However, our calculations confirm the presence of ETT and semiconductor to metal transition in β-AgBiSe$_2$ quite accurately using DFT (both at PBE and HSE06 levels), albeit, qualitatively.

The empirical results demonstrate that the significant enhancement of TE power has been observed in some materials during an ETT phenomenon.[9,10,23] For instance, ∼44% increase in TE power has been observed in p-type Sb$_{1.5}$Bi$_{0.5}$Te$_3$ in the vicinity of an ETT at ∼1.5 GPa.[23] Hence, it is worth to carry out the TE power measurement at high pressure on AgBiSe$_2$. Since the chemical pressure (chemical doping and substitutions) is analogous to the external pressure, it is experimentally possible to bring ETT at ambient conditions by proper alloying. Metallization under pressure can be used as the basis of pressure conducting (insulating) switches and sensors.[14,15] Hence our comprehensive studies propose that AgBiSe$_2$ can be used for the multilevel physics device with pressure sensors, pressure switches, and high thermoelectric performance at high pressure.

In summary, a combination of synchrotron XRD and the Raman scattering measurement confirms that AgBiSe$_2$

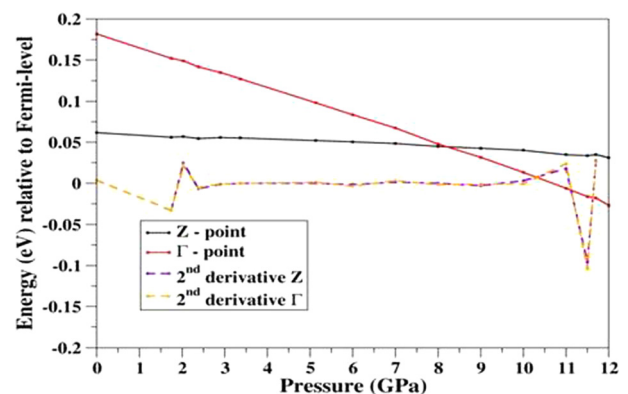FIG. 4. PDOS of β-AgBiSe$_2$ at pressure (a). 0 GPa and (b). 20 GPa.

FIG. 5. Variation of the conduction band position and its numerical second derivative at Γ and Z points with pressure.

undergoes the pressure induced weakly first order structural phase transition from hexagonal (P-3m1) to rhombohedral (R-3m) at $\sim$0.7 GPa. Furthermore, the $E_g^{(1)}$ and A_{1g} phonon mode frequency and line width anomaly due to the electron-phonon coupling changes along with the electrical transport measurement provide evidence for a pressure induced ETT at $\sim$2.8 GPa and a semiconductor to metal transition above 7 GPa. The first principles calculations corroborate the experimentally observed semiconductor to metal transition and suggest that the strong redistribution of electronic DOS mainly contributed by the p orbitals of Bi and Se atoms lying near to the Fermi level causes the metallization in β-AgBiSe$_2$. We are sure that our results will stimulate further research interest in AgBiSe$_2$ on the aspect of thermoelectric measurement at high pressure.

See supplementary material for the experimental, computational details, pressure coefficients, line width comparison of β-AgBiSe$_2$ with Bi$_2$Se$_3$, pressure dependent electronic band structure, and PDOS plots of β-AgBiSe$_2$.

[1] O. Gomis, R. Vilaplana, F. J. Manjón, P. Rodríguez-Hernández, E. Pérez-González, A. Muñoz, V. Kucek, and C. Drasar, Phys. Rev. B **84**, 174305 (2011).

[2] R. Vilaplana, O. Gomis, F. J. Manjón, A. Segura, E. Pérez-González, P. Rodríguez-Hernández, A. Muñoz, J. González, V. Marín-Borrás, V. Muñoz-Sanjosé, C. Drasar, and V. Kucek, Phys. Rev. B **84**, 104112 (2011).

[3] R. Vilaplana, D. Santamaría-Pérez, O. Gomis, F. J. Manjón, J. González, A. Segura, A. Muñoz, P. Rodríguez-Hernández, E. Pérez-González, V. Marín-Borrás, V. Muñoz-Sanjose, C. Drasar, and V. Kucek, Phys. Rev. B **84**, 184110 (2011).

[4] J. Zhang, C. Liu, X. Zhang, F. Ke, Y. Han, G. Peng, Y. Ma, and C. Gao, Appl. Phys. Lett. **103**, 052102 (2013).

[5] J. Zhang, Y. Han, C. Liu, X. Zhang, F. Ke, G. Peng, Y. Ma, and C. Gao, Appl. Phys. Lett. **105**, 062102 (2014).

[6] X. Xi, C. Ma, Z. Liu, Z. Chen, W. Ku, H. Berger, C. Martin, D. B. Tanner, and G. L. Carr, Phys. Rev. Lett. **111**, 155701 (2013).

[7] P. P. Kong, F. Sun, L. Y. Xing, J. Zhu, S. J. Zhang, W. M. Li, Q. Q. Liu, X. C. Wang, S. M. Feng, X. H. Yu, J. L. Zhu, R. C. Yu, W. G. Yang, G. Y. Shen, Y. S. Zhao, R. Ahuja, H. K. Mao, and C. Q. Jin, Sci. Rep. **4**, 6679 (2014).

[8] J. L. Zhang, S. J. Zhang, H. M. Weng, W. Zhang, L. X. Yang, Q. Q. Liu, S. M. Feng, X. C. Wang, R. C. Yu, L. Z. Cao, L. Wang, W. G. Yang, H. Z. Liu, W. Y. Zhao, S. C. Zhang, X. Dai, Z. Fang, and C. Q. Jin, Proc. Natl. Acad. Sci. U.S.A. **108**, 24 (2011).

[9] S. V. Ovsyannikov, V. V. Shchennikov, G. V. Vorontsov, A. Y. Manakov, A. Y. Likhacheva, and V. A. Kulbachinskii, J. Appl. Phys. **104**, 053713 (2008).

[10] N. V. Chandra Shekar, D. A. Polvani, J. F. Meng, and J. V. Badding, Phys. B **358**, 14 (2005).

[11] G. K. Pradhan, A. Bera, P. Kumar, D. Muthu, and A. Sood, Solid State Commun. **152**, 284 (2012).

[12] I. M. Lifshitz, Sov. Phys. JETP **11**, 1130 (1960).

[13] Y. A. Sorb, V. Rajaji, P. S. Malavi, U. Subbarao, P. Halappa, S. C. Peter, S. Karmakar, and C. Narayana, J. Phys.: Condens. Matter **28**, 015602 (2016).

[14] Z. Zhao, H. Zhang, H. Yuan, S. Wang, Y. Lin, Q. Zeng, G. Xu, Z. Liu, G. K. Solanki, K. D. Patel, Y. Cui, H. Y. Hwang, and W. L. Mao, Nat. Commun. **6**, 7312 (2015).

[15] A. P. Nayak, S. Bhattacharyya, J. Zhu, J. Liu, X. Wu, T. Pandey, C. Jin, A. K. Singh, D. Akinwande, and J. F. Lin, Nat. Commun. **5**, 3731 (2014).

[16] L. Pan, D. Bérardan, and N. Dragoe, J. Am. Chem. Soc. **135**, 4914 (2013).

[17] S. N. Guin, V. Srihari, and K. Biswas, J. Mater. Chem. A **3**, 648 (2015).

[18] C. Xiao, X. Qin, J. Zhang, R. An, J. Xu, K. Li, B. Cao, J. Yang, B. Ye, and Y. Xie, J. Am. Chem. Soc. **134**, 18460 (2012).

[19] G. V. P. Kumar and C. Narayana, Curr. Sci. **93**, 778 (2007).

[20] Y. M. Blanter, M. I. Kaganov, A. V. Pantsulaya, and A. A. Varlamov, Phys. Rep. **245**, 159 (1994).

[21] H. Takatsu, S. Yonezawa, S. Mouri, S. Nakatsuji, K. Tanaka, and Y. Maeno, J. Phys. Soc. Jpn. **76**, 104701 (2007).

[22] M. Cardona, High Pressure Res. **24**, 17 (2004).

[23] D. A. Polvani, J. F. Meng, N. V. Chandra Shekar, J. Sharp, and J. V. Badding, Chem. Mater. **13**, 2068 (2001).